# EMERGENCY SCENARIOS OF A RE-ENTRY VEHICLE DUE TO CONTROL DEGRADATION

O. da Costa and G. Sachs

Institute of Flight Mechanics and Flight Control, Technische Universität München
Munich, Germany

email: dacosta@lfm.mw.tum.de

## ABSTRACT

A controls degradation scenario is investigated for a reentry vehicle. It is assumed that one of two body flaps is blocked. The reaction control system is used to generate control moments in combination with the aerodynamic surfaces still operative. Particular emphasis is placed on implementing a control allocation method which yields an optimum utilization of the aerodynamic control surfaces in terms of minimizing the propellant mass required for the reaction control system. Minimum-propellant trajectories for the blocked body flap scenarios are determined using an efficient optimization technique. Results are presented which address blocked body flap scenarios caused by off-normal situations already in the orbital phase. The results show that no additional landing sites are required if an adequate amount of propellant mass is available.

## INTRODUCTION

For a space mission the ascent and reentry involve risks due to various failure possibilities in these phases. With regard to emergency scenarios, extreme thermal and mechanical loads on the vehicle during reentry require particular attention.

For the planned Crew Return Vehicle, concepts and strategies for safe mission aborts were developed in the German ASTRA Program (Selected Technologies for Future Space Transportation Systems). As preparatory work, systematic identification and classification of possible hazards and dangerous conditions during reentry have been performed. The goal was to provide emergency instructions and procedures (hazard reduction sequence including alternate trajectories) for hazard and risk reduction in order to ensure maximum mission safety in compliance with safety related guidelines (Refs. 1-3).

The evaluated scenario concerns blocking of a body flap that may be caused by off-normal situations already in the orbital phase. Due to the limited orbit duration of the vehicle (9 hours), deorbit and reentry have to be performed, instead of a safer "Safe Haven". Previous investigations show that maintaining the nominal flight path is not possible if a body flap is blocked (Ref. 4). Therefore appropriate emergency reentry trajectories including the deorbit maneuver have been determined as a means for coping with this problem.

## VEHICLE AND MISSION

The vehicle considered in this paper (Fig. 1) is a lifting body with a lift-to-drag ratio of about 0.9 during the hypersonic phase. Three different control options can be used, depending on the flight condition. The attitude control system is applied at altitudes above 90 km, providing moments by thrusters. Further, two body flaps are operated for the most part of the reentry, used in symmetrical and differential deflection modes (corresponding to elevator and aileron). Starting at a Mach number of $M = 6$, rudders which are mounted at the top of each fin can be additionally used for yaw control and as air brakes. All relevant vehicle parameters are listed in Table 1. The nominal landing site coordinates are shown in Table 2.

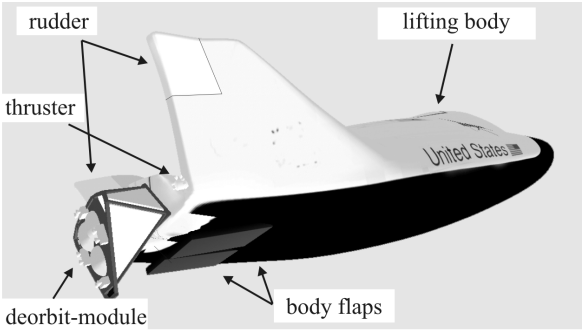


Fig. 1: Vehicle X-38

| Notation | |
|---|---|
| Vehicle mass $m$ [kg] | 1134 |
| Reference area $S$ [m²] | 22.7 |
| Maximum flap hinge moment $M_{hinge\max}$ [Nm] | 25881 |
| Maximum flap temperature $T_{flap\max}$ [°C] | 1750 |
| Deorbit module thrust $T_{deorbit}$ [N] | 4096 |

Table 1: Vehicle data

| Coober Pedy, Australia | |
|---|---|
| $\lambda_{CP} = 134.9°$ | $\delta_{CP} = -28.2°$ |
| Nequem, Argentina | |
| $\lambda_{NQ} = -68.94°$ | $\delta_{NQ} = -38.57°$ |
| San Nicolas Island, USA | |
| $\lambda_{SN} = -119.27°$ | $\delta_{SN} = 33.14°$ |

Table 2: Nominal landing site coordinates

## HAZARD SCENARIO

It is assumed that there is a blocked body flap scenario occurring in orbit, prior to reentry. The main goal is to enlarge the reentry window so that the number of landing sites can be kept as small as possible. A solution which would require only the nominal landing sites is of particular interest.

Between two subsequent orbit tracks, there is a displacement

$$\Delta\lambda = -2\pi \frac{\omega_E}{r_E}\sqrt{\frac{(r_E+h)^3}{g_0}} \tag{1}$$

For an orbit at the altitude of the ISS (386 km), the displacement amounts to $\Delta\lambda_{\min} = 23.09°$ (descending or ascending node). The time for an orbit can be expressed as

$$T_{co}(h) = \frac{2\pi}{r_E}\sqrt{\frac{(r_E+h)^3}{g_0}} \tag{2}$$

It is given by $T_{co} = 92.13$ min for the addressed orbit at an altitude of 386 km.

Assuming a maximum orbit duration of 9 hours, a total range of $\Delta\lambda_{\max} = 135.34°$ results. This means with regard to the hazardous scenarios that the three nominal landing sites can be reached for any initial condition if a minimum cross range capability of $\Delta\lambda_{\min}$ is available.

## MODELING OF VEHICLE DYNAMICS

A 6-degree-of-freedom model is used for describing the dynamics of the vehicle. The equations of motion read

$$\begin{aligned}
\dot{h} &= V\sin\gamma \\
\dot{\lambda} &= \frac{V\cos\gamma\cos\chi}{r_E+h} \\
\dot{\delta} &= \frac{V\cos\gamma\sin\chi}{(r_E+h)\cos\delta} \\
\dot{V} &= \frac{-D+T_{deorbit}\cos\alpha}{m} - g\sin\gamma + \omega_E{}^2(r_E+h)\cdot \\
&\quad \cdot\cos\delta(\sin\gamma\cos\delta - \cos\gamma\sin\delta\cos\chi) \\
\dot{\gamma} &= \frac{L+T_{deorbit}\sin\alpha}{mV}\cos\mu - \frac{Y}{mV}\sin\mu \\
&\quad + \cos\gamma\left(\frac{V}{(r_E+h)} - \frac{g}{V}\right) + 2\omega_E\cos\delta\sin\chi \\
&\quad + \frac{\omega_E{}^2(r_E+h)}{V}\cos\delta\cdot(\cos\gamma\cos\delta - \sin\gamma\sin\delta\cos\chi) \\
\dot{\chi} &= \frac{L}{mV\cos\gamma}\sin\mu + \frac{Y}{mV\cos\gamma}\cos\mu \\
&\quad + \frac{V\cos\gamma\sin\chi\tan\delta}{r} \\
&\quad - 2\omega_E\cdot(\tan\gamma\cos\delta\cos\chi - \sin\delta) \\
&\quad + \frac{\omega_E{}^2(r_E+h)}{V\cos\gamma}\sin\delta\cos\delta\sin\chi
\end{aligned} \tag{3}$$

and

$$\frac{d}{dt}\vec{\omega} = \mathbf{I}^{-1}\left(\vec{M}_c + \vec{M}_a - \vec{\omega}\times\mathbf{I}\vec{\omega}\right) \tag{4}$$

with matrix $\mathbf{I}$

$$\mathbf{I} = \begin{bmatrix} I_{xx} & 0 & -I_{xz} \\ 0 & I_{yy} & 0 \\ -I_{zx} & 0 & I_{zz} \end{bmatrix}$$

For describing the properties of the atmosphere, a model is used which is an approximation of the U.S Standard Atmosphere 1976.

Constraints are imposed on angle of attack, dynamic pressure, load factor and heat flux. A detailed description is given in Ref. 5.

## BLOCKED BODY FLAP SCENARIO

Successive dynamic inversion is applied to transform the equations of motion for the rotational dy-

namics into a system which is approximately linear. Additional feedback control provides tracking of the commands $\alpha_c$, $\beta_c$ and $\mu_c$. A detailed description of the optimization technique is given in Refs. 6 and 7.

Two phases are considered concerning operation of the rudders. Because of the high temperatures in the first phase, the rudders are set at a neutral position. The propellant mass rate can be calculated from the values of each thruster. It is given by the following relation

$$\dot{m}_{prop} = b_{th}\left(K_l \left| l_{thrust} \right| + K_m \left| m_{thrust} \right| + K_n \left| n_{thrust} \right|\right) \quad (5)$$

With

$$\begin{pmatrix} l_{thrust} \\ m_{thrust} \\ n_{thrust} \end{pmatrix} = \begin{pmatrix} l_c \\ m_c \\ n_c \end{pmatrix} - \begin{pmatrix} C_{l\delta_a}(\alpha,M)\,\delta_a\,\bar{q}SL \\ C_{m\delta_e}(\alpha,M)(\delta_e-\delta_{trim})\,\bar{q}SL \\ C_{n\delta_a}(\alpha,M)\,\delta_a\,\bar{q}SL \end{pmatrix} \quad (6)$$

and

$$\delta_a = \delta_e - \delta_{block} \quad (7)$$

Eq. (5) can be rewritten as

$$\begin{aligned} \dot{m}_{prop} = b_{th}\ \Big[ & K_l \left| l_c - C_{l\delta_a}(\delta_e - \delta_{block})\bar{q}SL \right| \\ & + K_m \left| m_c - C_{m\delta_e}(\delta_e - \delta_{trim})\,\bar{q}SL \right| \\ & + K_n \left| n_c - C_{n\delta_a}(\delta_e - \delta_{block})\bar{q}SL \right| \Big] \end{aligned} \quad (8)$$

Evaluation of Eq. (8) shows that the propellant mass rate has a minimum for an elevon deflection given by one of the following relations:

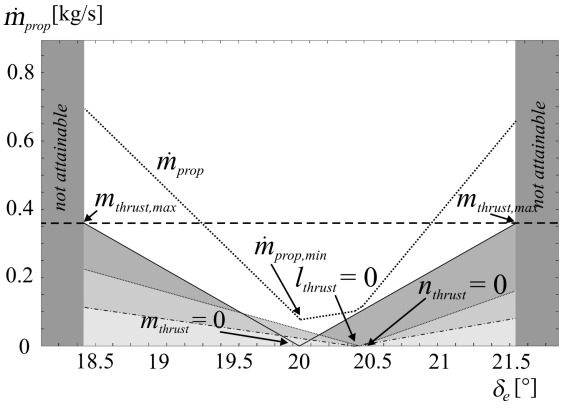


Fig. 2: Propellant mass rate in first phase

$$l_c - \left[ C_{l\delta_a}(\delta_{e1} - \delta_{block})\bar{q}SL \right] = 0 \quad (9a)$$

$$m_c - C_{m\delta_e}(\delta_{e2} - \delta_{trim})\bar{q}SL = 0 \quad (9b)$$

$$n_c - \left[ C_{n\delta_a}(\delta_{e3} - \delta_{block})\bar{q}SL \right] = 0 \quad (9c)$$

Fig. 2 presents an example for a blocked body flap deflection of 20° at Mach 20.

The application of the rudders below Mach 6 can be used to reduce the propellant mass required for generating control moments. This is illustrated in Fig. 3 which shows the propellant mass rate for a blocked body flap deflection of 20° at Mach 5.. The three lines for each of which a thruster moment is zero establish a triangle, corresponding to the following relations

$$l_c - \left[ C_{l\delta_a}(\delta_e - \delta_{block}) + C_{l\delta_r}\delta_r \right] \bar{q}SL = 0 \quad (10a)$$

$$m_c - C_{m\delta_e}(\delta_e - \delta_{trim})\,\bar{q}SL = 0 \quad (10b)$$

$$n_c - \left[ C_{n\delta_a}(\delta_e - \delta_{block}) + C_{n\delta_r}\delta_r \right] \bar{q}SL = 0 \quad (10c)$$

The minimum propellant mass rate is given by the lowest vertex ($\dot{m}_{prop,\min}$). A further description is given in Ref. 5.

The objective of the optimization is to keep the propellant mass as small as possible. Solutions have been obtained using the software system GESOP (Ref. 8).

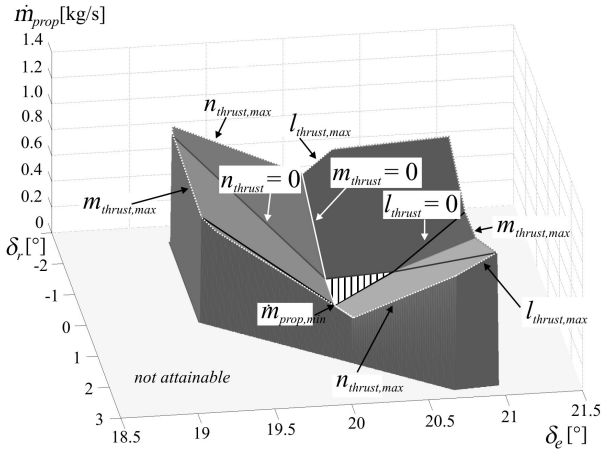


Fig. 3: Propellant mass rate in second phase

## RESULTS FOR BLOCKED BODY FLAP SCENARIO

Results are presented in Figs. 4 and 5 for a blocked body flap scenario of $\delta_{block} = 14°$. It is assumed that the maximum number of thrusters is available, corresponding to an enlargement of the system with 200 lbf thrusters. Fig. 4 shows the orbital and reentry trajectories for the earliest and latest possible descending node, reaching the nominal landing site Coober Pedy in Australia with a fuel consumption less than 100 kg. The difference between the earliest and latest descending node is determined by the maximum cross range capability of $\Delta\lambda_{descending\ node} = 27.6°$ for this scenario. Another possibility to reach Coober Pedy is to initiate the deorbit maneuver after passing an appropriate ascending node. But this alternative has the disadvantage that a great part of the trajectory takes place over inhabited territory.

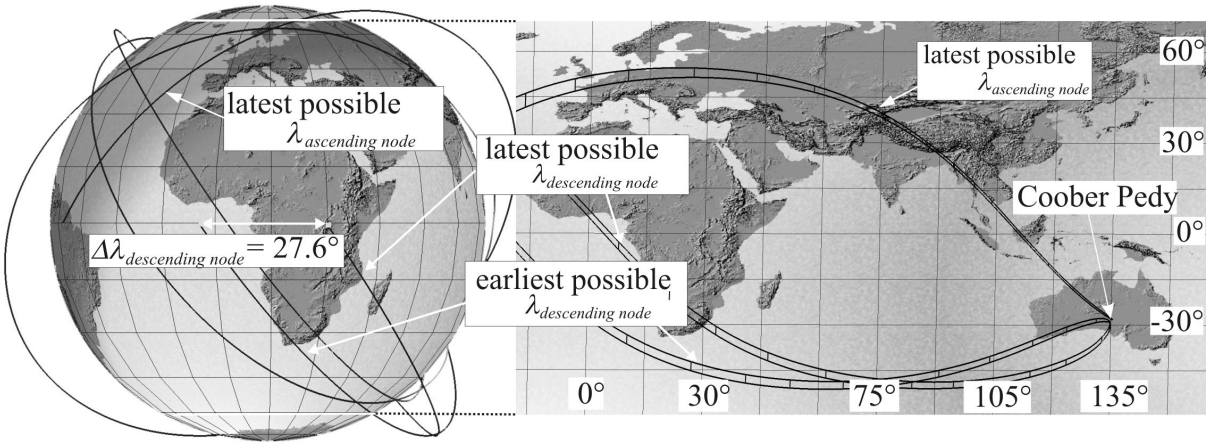


Fig. 4: Earliest and latest possible descending node to reach Coober Pedy, Australia, for a blocked body flap scenario with $\delta_{block} = 14°$, $m_{prop} = 100$ kg

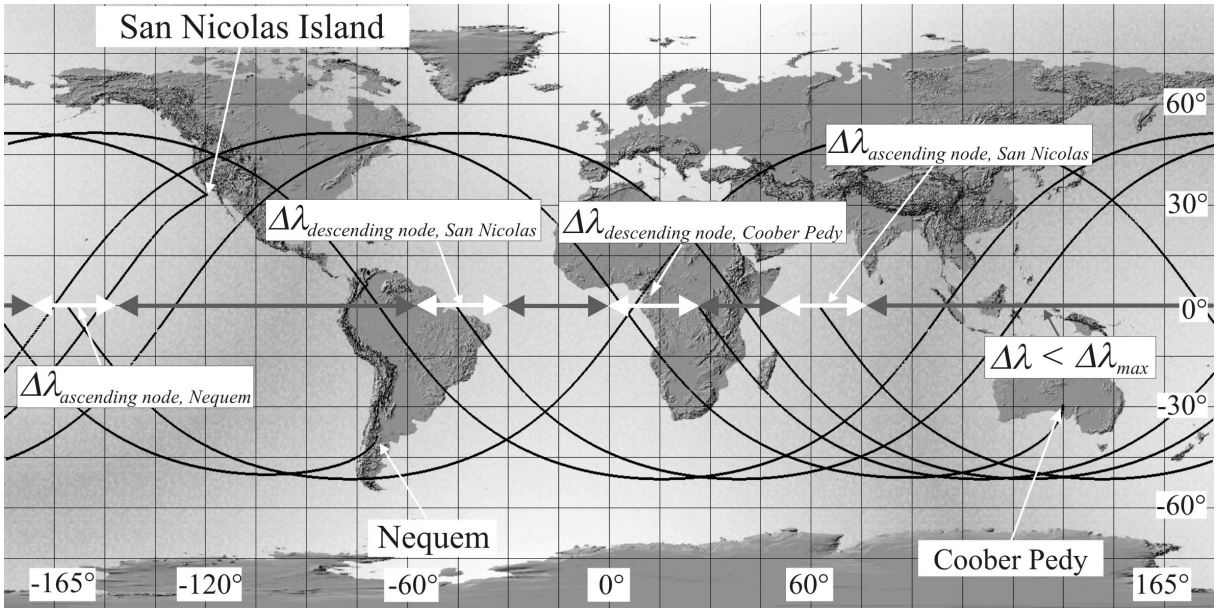


Fig. 5: Complete mission possibilities for blocked body flap scenario with $\delta_{block} = 14°$, $m_{prop} = 100$ kg

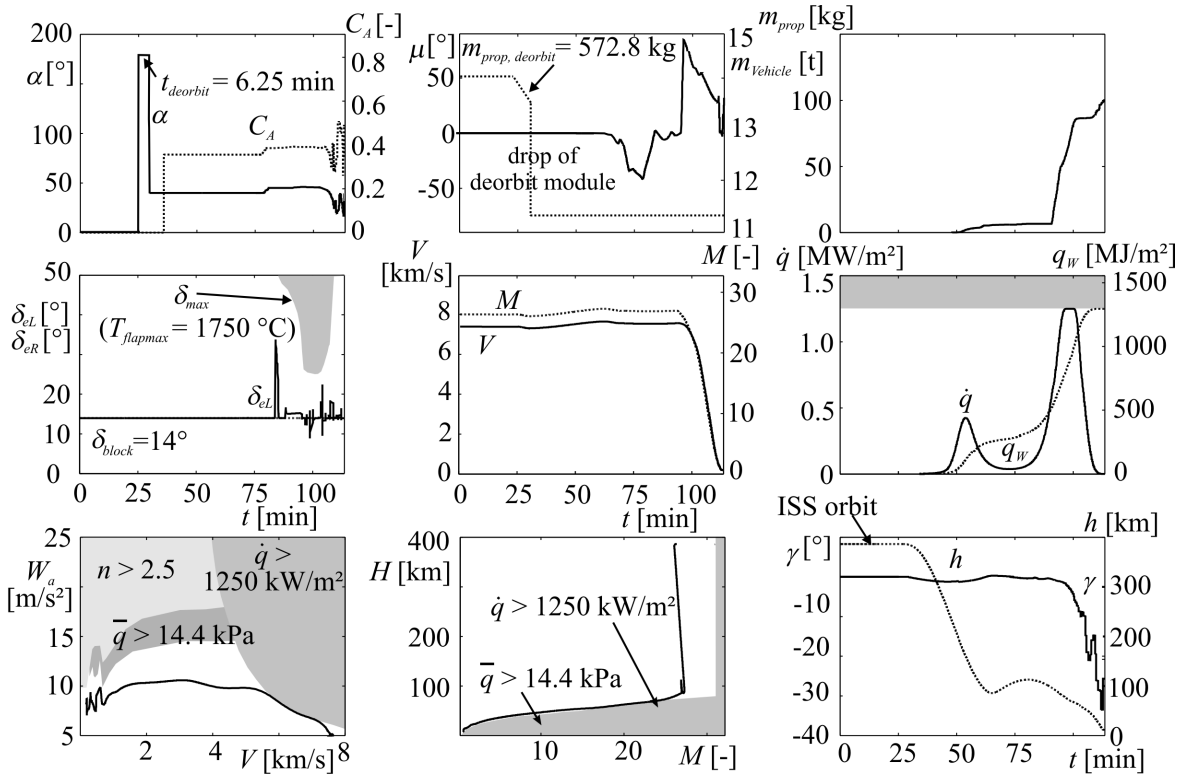


Fig. 6: Time histories of quantities relevant for blocked body flap scenario $\delta_{block} = 14°$, $m_{prop} = 100$ kg

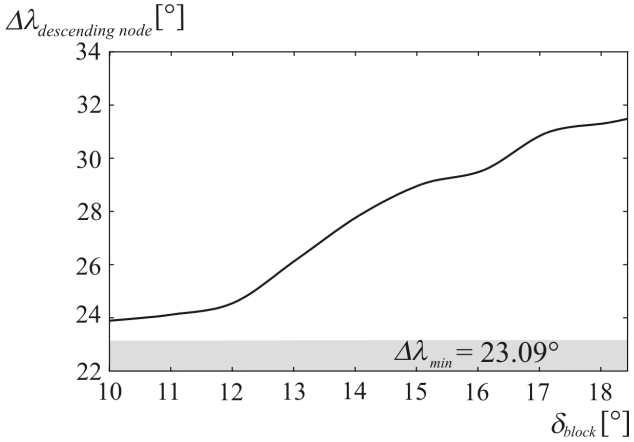


Fig. 7: Variation of blocked body flap scenarios with a maximum available propellant mass of $m_{prop} = 100$ kg.

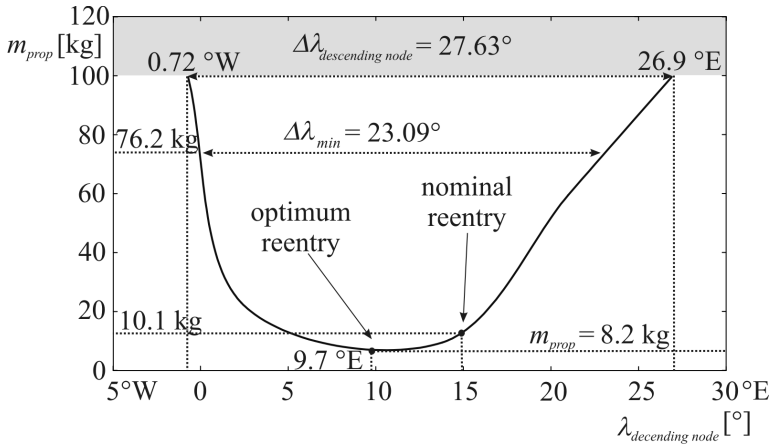


Fig. 8: Required propellant mass between earliest and latest possible descending node for $\delta_{block} = 14°$

Approaches to the other landing sites (San Nicolas Island, Nequem) are shown in Fig. 5 for the same hazardous scenario. The maximum time for staying in orbit before initiating the reentry occurs when the vehicle misses the possibility to approach San Nicolas Islands from the South (ascending node). Then the vehicle has to wait in orbit for about 7.1 hours to obtain an orbital displacement of 107° in westward direction before initiating the deorbit maneuver to reach Nequem from the South (ascending node).

Results are presented in Fig. 6 which shows the time histories of quantities relevant for this emergency scenario. Basically, the emergency scenario can be successfully coped with by aligning the remaining body flap with the blocked one and using the thrusters for generating control moments in yaw and roll. The commanded angle of attack has to be increased resulting in a lower cross range capability (nominal value $\Delta\lambda_{descending\ node}$ = 35°). The heat flux and heat load values are reaching their limits. Thus, a propellant mass of $m_{prop}$ = 100 kg is sufficient for this hazardous scenario.

Fig. 7 shows a variation of blocked body flap scenarios with an available propellant mass of $m_{prop}$ = 100 kg. For all analyzed blocked body flap scenarios, the cross range capability is sufficient with respect to $\Delta\lambda_{\min}$. The reason for a reduced cross range capability at lower blocked body flap positions originates from the turn at higher necessary angles of attack. But even for the lowest blocked body flap scenario analyzed ($\delta_{block}$ = 10°) a safety margin in cross range capability remains.

For the intermediate range between earliest and latest possible descending node, the amount of propellant mass required to reach Coober Pedy for a blocked body flap scenario of $\delta_{block}$ = 14° can be lowered to a minimum of $m_{prop}$ = 8.2 kg. Trajectory optimization with regard to changed initial conditions yields results as presented in Fig. 8. This Fig. also shows the values concerning blocked body flap scenarios for the nominal case as well as for the optimum reentry related to the descending node.

## CONCLUSIONS

A hazard scenario of a reentry vehicle is treated, concerning blocking of a body flap in the orbital phase before reentry. The reaction control system is considered to be used for generating control moments in combination with the aerodynamic control surfaces still operative after the failure has occurred. A trajectory optimization is performed for minimizing the propellant mass required by the thrusters for reaching one of the three nominal landing sites. Results are presented for various blocked body flap scenarios concerning the maximum cross range. The results show that no additional landing sites are required if some extra adequate amount of propellant mass can be used. Furthermore, the effects of the available amount of propellant mass concerning the cross range capability are considered.

## REFERENCES


1 N. N.: Hazard Analysis and Safety Risk Assessment – Methods and Procedures. ESA PSS-01-403, Issue 1, January 1994.

2 N. N.: System Safety Guidelines for Hazard Identification and Control – Systems Oriented Guide for Safety Engineers. JSC 11123, April 1992.

3 N. N.: NASA Safety Manual. NASA NSTS 1700.7B, Internet 2000.

4 da Costa, O., Sachs, G.: Effects of Controls Degradation on Flight Mission of Reentry Vehicle. AIAA Guidance, Navigation and Control Conference, Monterey, CA, USA, August 5-8, 2002, AIAA-2002-4848.

5 da Costa, O., Sachs, G.: Mission Abort Scenarios of a Reentry Vehicle with Controls Degradation, AIAA Guidance, Navigation and Control Conference, Austin, TX. USA, 11. - 14. August 2003, AIAA-2003-5735, 2003.

6 Wiegand, A., Markl, A., Mehlem, K.; Ortega, G., Steinkopf, M., Well, K.: ALTOS – ESA´s Trajectory Optimization Tool Applied to X-38 Reentry Vehicle Trajectory Design. IAF-99-A6.09.

7 Roenneke, A., Well, K.: Nonlinear Flight Control for a High Lift Reentry Vehicle. AIAA Paper 95-3370,1995.

8 N. N.: GESOP (Graphical Environment for Simulation and Optimization), Softwaresystem für die Bahnoptimierung. Institut für Robotik und Systemdynamik, DLR Oberpfaffenhofen, 1993.